Contribution from the Department of Chemistry, School of Science and Engineering, Waseda University, Tokyo 160, Japan, Department of Chemistry, Faculty of Science, Josai University, Sakado, Saitam 350-02, Japan, and National Chemical Laboratory for Industry, Higashi, Tsukuba, Ibaraki 305, Japan

Crystal Structure and ^{13}C and ^{195}Pt NMR Spectra of an α-Pyrrolidonate-Bridged Binuclear Platinum(II) Complex, $[Pt_2(NH_3)_4(C_4H_6NO)_2]_2(PF_6)_3(NO_3)\cdot H_2O$

Kazuko Matsumoto,*,† Hiroshi Miyamae,‡ and Hiroshi Moriyama§

Received May 26, 1988

The crystal structure and ^{13}C and ^{195}Pt NMR spectra of the amidate-bridged binuclear Pt(II) complex $[Pt_2(NH_3)_4(C_4H_6NO)_2]_2(PF_6)_3(NO_3)\cdot H_2O$ show that although the complex cation is binuclear in solution, it is tetranuclear in the solid state, where its structure is basically identical with that of the previously reported *cis*-diammineplatinum α-pyrrolidonate tan cation $[Pt_4(NH_3)_8(C_4H_6NO)_4]^{6+}$. The amidate-bridged Pt–Pt distance in the present complex is 3.033 (2) Å, and the central Pt–Pt distance, without the amidate bridge, is 3.186 (2) Å. These distances are significantly longer than the corresponding ones already reported for the α-pyridonate complexes $[Pt_2(NH_3)_4(C_5H_4NO)_2]_2^{4+}$ and $[Pt_2(en)_2(C_5H_4NO)_2]_2^{4+}$. Both ^{13}C and ^{195}Pt NMR spectra of the present complex in D_2O revealed the existence of head-to-head (H-H) and head-to-tail (H-T) isomers, indicating that the H-H isomer very rapidly isomerizes to the H-T isomer on dissolution in water and both isomers exist in equilibrium in solution. This rapid isomerization contrasts to the case of the corresponding α-pyridonate complex $[Pt_2(en)_2(C_5H_4NO)_2]^{2+}$, whose isomerization equilibrium requires about 2 days to be established.

Introduction

A few years ago, K.M. reported a rapid and convenient method for preparing an α-pyrrolidonate-bridged Pt(II) binuclear complex, $[Pt_2(NH_3)_4(C_4H_6NO)_2]^{2+}$.[1] The method utilizes the novel reduction reaction of the tetranuclear *cis*-diammineplatinum α-pyrrolidonate tan cation $[Pt_4(NH_3)_8(C_4H_6NO)_4]^{6+}$[2] with OH^-. The resulting binuclear cation, $[Pt_2(NH_3)_4(C_4H_6NO)_2]^{2+}$, was characterized by IR spectroscopy, elemental analyses, and solution conductivity studies, and its binuclear nature was concluded.[1] Concerning a similar amidate-bridged binuclear Pt(II) complex, α-pyridonate-bridged *cis*-diammineplatinum(II), $[Pt_2(NH_3)_4(C_5H_4NO)_2]^{2+}$, two isomers have been reported: head-to-head (H-H) and head-to-tail (H-T).[3] Both isomers are prepared from the reactions of *cis*-$[Pt(NH_3)_2(H_2O)](NO_3)_2$ with α-pyridone in water. Analogous isomers are also reported for the corresponding ethylenediamine complex, $[Pt_2(en)_2(C_5H_4NO)_2]^{2+}$, and novel linkage isomerization of H-H to H-T in water is observed with ^{195}Pt NMR spectroscopy.[4] The isomerization rates of the complex cations are strikingly different between the two complexes. H-H *cis*-$[Pt_2(NH_3)_4(C_5H_4NO)_2]^{2+}$ shows much slower isomerization than H-H $[Pt_2(en)_2(C_5H_4NO)_2]^{2+}$.[4] The X-ray crystal structure of the binuclear (ethylenediamine)platinum(II) cation revealed pronounced torsional strain and increased metal–metal distance relative to the *cis*-diammineplatinum(II) analogue.[4,5] These distortions seem to alter the lability of the platinum(II)–α-pyridonate bonds, resulting in a dramatic enhancement in the rate of linkage isomerization of the bridging α-pyridonate ligand.[4]

In the present study, the crystal structure and ^{13}C and ^{195}Pt NMR spectra of another amidate-bridged binuclear platinum(II) cation is reported. The amidate ligand in this study is α-pyrrolidonate, and the effect of the amidate ligand on the structure and H-H to H-T isomerization is discussed relative to that of the previously reported α-pyridonate analogue.

Experimental Section

Preparation of the Compound. The preparation procedure of the compound is basically the same as reported previously[1] and is as follows: A 50-mg sample of $[Pt_4(NH_3)_8(C_4H_6NO)_4](NO_3)_6\cdot 2H_2O$[2,9] was dissolved in 10 mL of water. After 60 mg of $NaPF_6$ was added to the solution, 2.4 M NaOH was gradually added to the solution until it turned completely yellow. The solution was left at room temperature, and brownish yellow rectangular crystals were obtained after a few days. Anal. Calcd for $[Pt_2(NH_3)_4(C_4H_6NO)_2]_2(PF_6)_3(NO_3)\cdot H_2O$: C, 10.87; H, 2.86; N, 10.30. Found: C, 10.91; H, 2.98; N, 10.28. The yield was about 20%. The crop seemed uniform microscopically, and IR and ^{195}Pt NMR spectra of the compound showed no difference from batch to batch. At least up to 20% yield, the crystals were H-H isomers.

Table I. Experimental Details of the X-ray Diffraction Study of $[Pt_2(NH_3)_4(C_4H_6NO)_2]_2(PF_6)_3(NO_3)\cdot H_2O$

(A) Crystal Parameters	
a = 18.571(3) Å	monoclinic
b = 21.019(5) Å	space group $C2/c$
c = 13.854(2) Å	Z = 4
β = 122.52(1)°	ρ(calcd) = 2.60 g cm^{-3}
V = 4560.0(16) Å^3	ρ(obsd)[a] = 2.62 g cm^{-3}
μ = 12.6 mm^{-1}	MW = 1786.0

(B) Measurement of Intensity Data	
instrument	Rigaku AFC-5 four-circle diffractometer
radiation	Mo Kα (λ = 0.7107 Å), graphite monochromatized
scan mode	ω–2θ
scan width	ω = (1.1 + 0.5 tan θ)°
2θ limit	$2° < 2\theta < 60°$
scan rate	4.0°/min in ω
stds	3 reflcns measd every 100 measurements, showing random, statistical fluctuations within 1.5%
no. of reflcns collcd	5388
no. of reflcns used for calcn	3544 unique reflcns for which $\lvert F_o\rvert > 3\sigma\lvert F_o\rvert$
data processing	Lorentz–polarization and abs cor

[a] By suspension in a mixture of $CHBr_3$ and $CHCl_3$.

Collection and Reduction of X-ray Data. The single crystal of the compound used for intensity measurement was approximately 0.2 × 0.2 × 0.1 mm. Unit cell parameters were obtained from a least-squares fit of 27 reflections in the range of $28° < 2\theta < 33°$ measured on a Rigaku AFC-5 four-circle diffractometer using graphite-monochromated Mo Kα radiation. The details of the data collection are presented in Table I.

Solution and Refinement of the Structure. The coordinates of the two platinum atoms were found from a Patterson map, and a series of block-diagonal least-squares refinements followed by Fourier-synthesis revealed all the remaining atoms except hydrogen atoms. The structure was finally refined with anisotropic temperature factors for all the atoms except hydrogen atoms to the final discrepancy indexes $R_1 = 0.104$ and $R_2 = 0.084$, where $R_1 = \sum\lvert\lvert F_o\rvert - \lvert F_c\rvert\rvert/\sum\lvert F_o\rvert$ and $R_2 = [\sum w_i\lvert\lvert F_o\rvert - \lvert F_c\rvert\rvert^2/\sum w_i\lvert F_o\rvert^2]^{1/2}$ ($w_i = (\sigma^2 + 0.02\lvert F_o\rvert^2)^{1/2}$). Calculated hydrogen pos-

† Waseda University.
‡ Josai University.
§ National Chemical Laboratory for Industry.

(1) Matsumoto, K.; Matoba, N. *Inorg. Chim. Acta* **1986**, *120*, L1.
(2) Matsumoto, K.; Fuwa, K. *J. Am. Chem. Soc.* **1982**, *104*, 897.
(3) Hollis, L. S.; Lippard, S. J. *J. Am. Chem. Soc.* **1983**, *105*, 3494.
(4) O'Halloran, T. V.; Lippard, S. J. *J. Am. Chem. Soc.* **1983**, *105*, 3341.
(5) Hollis, L. S.; Lippard, S. J. *Inorg. Chem.* **1983**, *22*, 2600.
(6) *International Tables for X-ray Crystallography*; Kynoch Press: Birmingham, England, 1974; Vol. IV.
(7) Sakurai, T.; Kobayashi, K. *Rikagaku Kenkyusho Hokoku* **1979**, *55*, 69.
(8) Johnson, C. K. Report ORNL-3794 (revised); Oak Ridge National Laboratory: Oak Ridge, TN, 1976.
(9) Matsumoto, K.; Takahashi, H.; Fuwa, K. *Inorg. Chem.* **1983**, *22*, 4086.

0020-1669/89/1328-2959$01.50/0

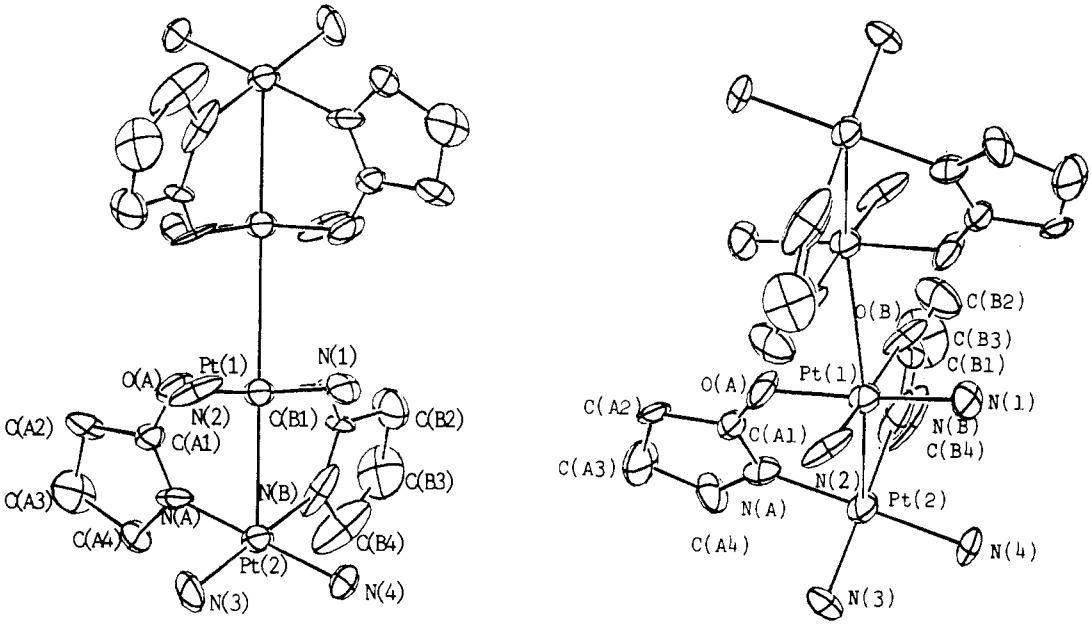

Figure 1. Molecular structure of $[Pt_2(NH_3)_4(C_4H_6NO)_2]_2^{4+}$ observed from two different angles. The molecule has an inversion center at the midpoint of the Pt(1)–Pt(1′) vector. Thermal ellipsoids are drawn at 50% probability.

itions for the ligands were included in the final structure factor calculation. No additional hydrogen atoms were included in the lattice. Atomic scattering factors were taken from ref 7. All the calculations were performed with the program systems UNICS-III[7] and ORTEP.[8]

The final positional and thermal parameters are listed in Table II. The observed and calculated structure factors (Table S1) and anisotropic temperature factors (Table S2) are available as supplementary material.

^{13}C and ^{195}Pt NMR Measurements. The ^{195}Pt NMR spectrum was acquired on a JEOL FX90A spectrometer. The measurement was performed at 19.21 MHz. Since the 90° pulse was 16 μs, a 25° pulse (4 μs) was adopted for accumulation. ^{13}C NMR spectra were aquired on both a Bruker AC200P and a JEOL FX90A spectrometer, at 50.3 and 22.5 MHz, respectively.

NMR measurements were performed both for a saturated solution of H-H $[Pt_2(NH_3)_4(C_4H_6NO)_2]_2(PF_6)_3(NO_3)\cdot H_2O$ in D_2O and for a saturated solution in situ prepared by dissolving $[Pt_4(NH_3)_8(C_4H_6NO)_2](NO_3)_6\cdot 2H_2O$ in D_2O and reducing it with 2.4 M NaOH. All the sample dissolutions were carried out at room temperature. Both solutions gave identical ^{13}C and ^{195}Pt NMR spectra; however, the S/N ratio was better for the latter solution due to higher solubility of the compound. All the spectra reported in this paper are for the latter solution. Chemical shift data for ^{13}C NMR spectroscopy are reported relative to TMS, which is set in a sealed coaxial capillary tube in a 5-mm sample tube, whereas a saturated solution of $PtCl_6^{2-}$ in D_2O was used as an external reference for ^{195}Pt chemical shift data. All chemical shifts are expressed in ppm, and coupling constants, in Hz. Sample temperature was regulated on a Bruker AC200P spectrometer at 25 °C by using a variable-temperature controller.

Results and Discussion

Description of the Structure. As shown in Figure 1, the cation exists as a tetranuclear complex composed of two binuclear, α-pyrrolidonate-bridged moieties related through a crystallographic inversion center that lies at the midpoint of the Pt(1)–Pt(1′) vector. The tetranuclear structure is basically identical with those of the so far reported α-pyrrolidone tan,[2,9] green,[10] and violet complexes,[11,12] the difference between them being the average platinum oxidation state. The distance between the α-pyrrolidonate-bridged platinum atoms Pt(1) and Pt(2) of 3.029 (2) Å is 0.155 Å shorter than the inner Pt(1)–Pt(1′) distance of 3.184 (2) Å. Table III

Table II. Atomic Parameters[a]

atom	x	y	z	B_{EQV}
Pt(1)	2325 (1)	1833 (0)	382 (1)	3.06 (0.04)
Pt(2)	2173 (1)	877 (1)	1899 (1)	3.63 (0.04)
P(A)	5000	203 (6)	7500	5.57 (0.56)
P(B)	1223 (5)	1500 (4)	−4047 (7)	4.52 (0.34)
N(0)	0	298 (15)	−2500	11.41 (2.53)
O(N1)	−504 (18)	470 (16)	−3361 (22)	13.98 (1.72)
O(N2)	0	−80 (23)	−2500	21.34 (3.47)
N(1)	2865 (14)	1389 (11)	−345 (18)	4.93 (1.14)
N(2)	1174 (12)	1829 (10)	−1135 (15)	3.94 (0.81)
N(3)	917 (12)	550 (10)	785 (19)	5.06 (1.01)
N(4)	2668 (13)	25 (10)	1599 (22)	5.89 (1.21)
O(A)	1762 (11)	2367 (8)	1010 (14)	4.18 (0.82)
N(A)	1730 (13)	1673 (12)	2247 (19)	5.35 (1.10)
C(A1)	1623 (14)	2243 (11)	1742 (19)	3.30 (0.98)
C(A2)	1222 (18)	2709 (13)	2178 (25)	5.09 (1.48)
C(A3)	1323 (21)	2356 (17)	3228 (26)	6.73 (1.75)
C(A4)	1552 (20)	1657 (18)	3117 (23)	7.54 (1.68)
O(B)	3495 (10)	1889 (8)	1791 (13)	4.10 (0.70)
N(B)	3366 (13)	1179 (9)	2954 (17)	4.10 (0.96)
C(B1)	3781 (14)	1579 (11)	2731 (19)	2.95 (0.94)
C(B2)	4675 (15)	1670 (10)	3729 (20)	3.92 (1.01)
C(B3)	4757 (18)	1234 (15)	4598 (23)	6.40 (1.31)
C(B4)	3879 (15)	978 (12)	4164 (20)	3.85 (1.06)
W(1)	2222 (15)	−20 (11)	4101 (20)	8.43 (1.32)
F(A1)	4305 (15)	696 (11)	6681 (19)	11.33 (1.41)
F(A2)	5385 (12)	193 (10)	6731 (15)	8.42 (1.07)
F(A3)	4364 (13)	−345 (10)	6767 (20)	11.57 (1.35)
F(B1)	456 (14)	1617 (10)	−3900 (21)	10.61 (1.52)
F(B2)	1415 (17)	2156 (11)	−3975 (38)	21.27 (2.97)
F(B3)	1951 (14)	1367 (12)	−4241 (20)	10.71 (1.42)
F(B4)	1856 (16)	1403 (17)	−2828 (16)	16.49 (1.61)
F(B5)	583 (17)	1591 (16)	−5296 (20)	15.48 (1.58)
F(B6)	967 (13)	810 (9)	−4218 (29)	16.01 (2.05)
H(A1)	55	280	150	7.5
H(A2)	156	317	239	7.5
H(A3)	72	240	321	7.5
H(A4)	181	260	402	7.5
H(A5)	102	134	292	7.5
H(A6)	210	150	395	7.5
H(B1)	477	216	401	7.0
H(B2)	512	156	347	7.0
H(B3)	503	149	541	7.0
H(B4)	521	86	473	7.0
H(B5)	365	118	468	7.0
H(B6)	391	46	427	7.0

[a] Positional Parameters are multiplied by 10^4. Thermal parameters are given by the equivalent temeprature factors (Å^2).

(10) Matsumoto, K.; Takahashi, H.; Fuwa, K. *J. Am. Chem. Soc.* **1984**, *106*, 2049.
(11) Matsumoto, K.; Fuwa, K. *Chem. Lett.* **1984**, 569.
(12) Matsumoto, K. *Bull. Chem. Soc. Jpn.* **1985**, *58*, 65.
(13) Laurent, J.-P.; Lepage, P.; Dahan, F. *J. Am. Chem. Soc.* **1982**, *104*, 7335.
(14) Barton, J. K.; Szalda, D. J.; Rabinowitz, H. N.; Waszczak, J. V.; Lippard, S. J. *J. Am. Chem. Soc.* **1979**, *101*, 1434.

Table III. Geometric Comparison of Amidate-Bridged Tetranuclear Platinum Complexes

compd	av Pt oxidn state	Pt–Pt, Å	τ,[a] deg	ω,[a] deg	Pt–Pt–Pt, deg	ref
α-pyrrolidonate (yellow)	+2.0	3.033 (2)[d]	35.9	17.9	157.85 (8)	*b*
$[Pt_2(NH_3)_4(C_4H_6NO)_2](PF_6)_3(NO_3)\cdot 2H_2O$		3.186 (2)				
1-methylhydantoinate (yellow)	+2.0	3.131[d]	*c*	*c*	160.5	13
$[Pt_2(NH_3)_4(C_4H_5N_2O_2)_2]_2(NO_3)_4\cdot H_2O$		3.204				
α-pyridonate (yellow)	+2.0	2.8767 (7)[d]	30.0	20.3	158.40 (3)	3
$[Pt_2(NH_3)_4(C_5H_4NO)_2]_2(NO_3)_4$		3.1294 (4)				
α-pyridonate (yellow)	+2.0	2.992 (1)[d]	39.6	24.9	160.58 (3)	5
$[Pt_2(en)_2(C_5H_4NO)_2]_2(NO_3)_4$		3.236 (1)				
α-pyridonate (blue)	+2.25	2.7445 (4)[d]	27.4	22.8	164.60 (2)	14
$[Pt_4(NH_3)_8(C_5H_4NO)_4](NO_3)_5\cdot H_2O$		2.8770 (9)				
α-pyridonate (blue)	+2.25	2.8296 (5)[d]	32.1	24.3	164.33 (3)	15
$[Pt_4(en)_4(C_5H_4NO)_4](NO_3)_5\cdot H_2O$		2.9158 (5)				
α-pyrrolidonate (tan)	+2.5	2.702 (6)[d]	18.7	4.3	170.4 (1)	9
$[Pt_4(NH_3)_8(C_4H_6NO)_4](NO_3)_6\cdot 2H_2O$		2.710 (5)	21.2	5.1	168.8 (1)	
		2.705 (6)[d]				

[a] τ is the tilt angle between adjacent Pt-coordination planes in the ligand bridging unit, and ω is the torsion angle about the Pt–Pt vector. [b] This work. [c] Value not reported. [d] Bridged Pt–Pt distance.

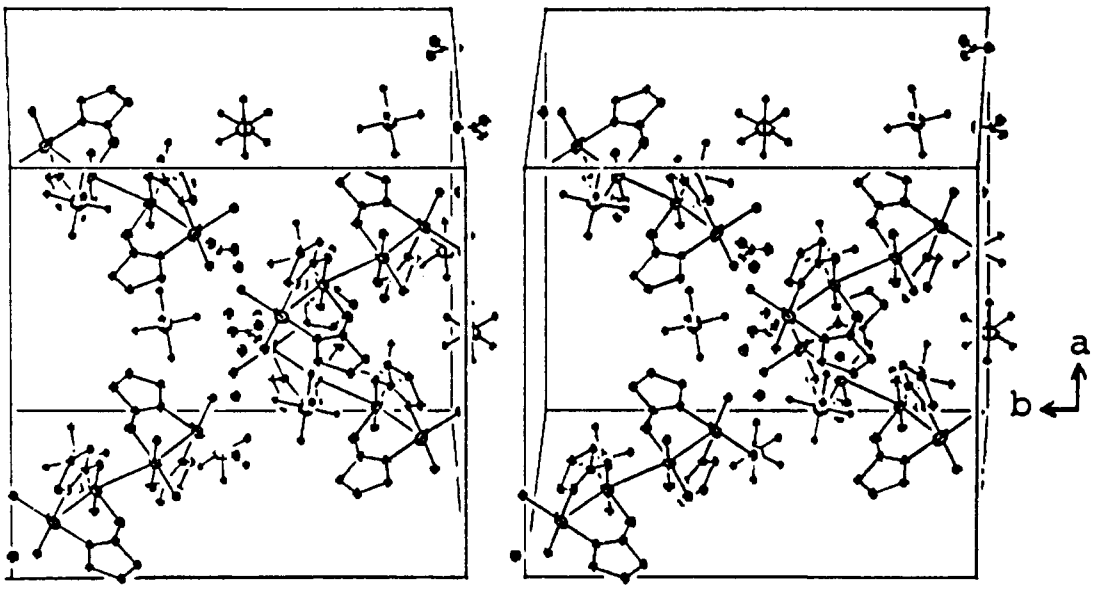

Figure 2. Crystal structure of $[Pt_2(NH_3)_4(C_4H_6NO)_2]_2(PF_6)_3(NO_3)\cdot H_2O$ viewed along the c^* axis.

summarizes geometric comparisons of related tetranuclear complexes. The two Pt–Pt distances in the present complex are 0.3–0.4 Å longer than the corresponding ones in the *cis*-diammineplatinum α-pyrrolidonate tan cation with platinum in the +2.5 average oxidation state. The relation that the Pt–Pt distance increases with decreasing average platinum oxidation state is widely observed in this class of compounds.[10] The two Pt–Pt distances in the present complex are even longer (ca. 0.16 Å) than those in the corresponding (α-pyridonato)platinum(II) complex, but shorter than those reported for the (1-methylhydantoinato)platinum(II) complex (Table III). The angle between the Pt(2)–Pt(1) and Pt(1)–Pt(1′) vectors in the four-atom zigzag chain is 157.85 (8)°. Both coordination planes around Pt(1) and Pt(2) intersect with the Pt(1)–Pt(2) vector at angles of 69.8 and 74.3°, respectively. The coordination plane of Pt(1) is almost perpendicular to the Pt(1)–Pt(1′) vector (87.2°). Bond distances and angles shown in Table IV within the platinum coordination planes compare favorably with values found in related α-pyridonate- or α-pyrrolidonate-bridged tetranuclear complexes[3,5,9,10] of platinum in the +2, +2.25, or +2.5 average oxidation state. The Pt–N(amine) distances trans to the pyrrolidonate nitrogen atoms are slightly longer (0.1 Å) than those trans to the pyrrolidonate oxygen atoms. The same tendency is observed in reported amidate-bridged tetranuclear complexes and indicates a larger trans influence of the heterocyclic nitrogen atom than of the oxygen atom in amidate ligands.[15] A recent SCF–Xα calculation on *cis*-diammineplatinum α-pyridone blue revealed that the trans influence originates in a more extensive σ-overlap of the Pt–N(heterocycle) bond relative to the Pt–O(amidate) bond.[16]

Both platinum coordination spheres are planar with four-atom root-mean-square deviations of 0.01 Å for the Pt(1) plane and 0.02 Å for the Pt(2) plane. As observed in all the platinum blue complexes regardless of the platinum oxidation state, the platinum atoms are slightly displaced out of the coordination planes toward one another, by 0.10 Å for Pt(1) and 0.2 Å for Pt(2). Comparison of the bond lengths and angles within the two α-pyrrolidonate rings shows that both rings are equivalent and have the usual geometries, compared to the α-pyrrolidonate tetranuclear complex of platinum in the +2.5 average oxidation state.[2,9]

Hydrogen bonds connecting the two binuclear subunits across the inversion center occur at N(1)–O(A′) and N(2)–O(B′). The crystal packing of the cations and anions is shown in Figure 2. The tetranuclear units are further linked through a network of hydrogen bonds between the amine ligands and nitrate anions. Oxygen atom W(1) of the crystal water is 3.54 (3) Å from Pt(2) at the end of the tetranuclear Pt_4 chain. All P–F bond distances within the PF_6^- anions are normal.

Structural Comparisons among Amidate-Bridged Tetranuclear Platinum Complexes. Table III lists structural features of platinum blue ($Pt^{2.25+}$ average oxidation state), yellow ($Pt^{2.0+}$ average oxidation state), and tan complexes ($Pt^{2.5+}$ average oxidation state) with α-pyridonate or α-pyrrolidonate ligands. While the distances

(15) O'Halloran, T. V.; Mascharak, P. K.; Williams, I. D.; Roberts, M. M.; Lippard, S. J. *Inorg. Chem.* **1987**, *26*, 1261.

(16) Ginsberg, A. P.; O'Halloran, T. V.; Fanwick, P.; Hollis, L. S.; Lippard, S. J. *J. Am. Chem. Soc.* **1984**, *106*, 5430.

Table IV. Bond Distances (Å) and Angles (deg)[a]

(A) $[(Pt_2(NH_3)_4(C_4H_6NO)_2]_2^{4+}$ Cation			
Pt(1)-Pt(2)	3.029 (2)	Pt(1)-Pt(1^i)	3.184 (2)
Pt(1)-N(1)	2.00 (3)	Pt(2)-N(3)	2.10 (2)
Pt(1)-N(2)	2.04 (1)	Pt(2)-N(4)	2.15 (2)
Pt(1)-O(A)	2.02 (2)	Pt(2)-N(A)	2.03 (3)
Pt(1)-O(B)	2.00 (1)	Pt(2)-N(B)	1.99 (2)
O(A)-C(A1)	1.20 (4)	O(B)-C(B1)	1.29 (3)
N(A)-C(A1)	1.34 (3)	N(B)-C(B1)	1.28 (4)
N(A)-C(A4)	1.41 (5)	N(B)-C(B4)	1.48 (3)
C(A1)-C(A2)	1.54 (5)	C(B1)-C(B2)	1.50 (3)
C(A2)-C(A3)	1.55 (5)	C(B2)-C(B3)	1.45 (4)
C(A3)-C(A4)	1.56 (5)	C(B3)-C(B4)	1.50 (4)
Pt(2)-Pt(1)-Pt(1^i)	157.94 (5)		
Pt(2)-Pt(1)-N(1)	107.4 (7)	Pt(1)-Pt(2)-N(3)	100.8 (7)
Pt(2)-Pt(1)-N(2)	106.0 (7)	Pt(1)-Pt(2)-N(4)	102.1 (8)
Pt(2)-Pt(1)-O(A)	78.9 (5)	Pt(1)-Pt(2)-N(A)	79.5 (8)
Pt(2)-Pt(1)-O(B)	79.6 (6)	Pt(1)-Pt(2)-N(B)	79.4 (7)
Pt(1^i)-Pt(1)-N(1)	89.8 (7)	Pt(1^i)-Pt(1)-N(2)	87.1 (6)
Pt(1^i)-Pt(1)-O(A)	84.3 (6)	Pt(1^i)-Pt(1)-O(B)	88.0 (5)
N(1)-Pt(1)-N(2)	90.6 (8)	N(3)-Pt(2)-N(4)	90.4 (8)
N(1)-Pt(1)-O(A)	173.7 (9)	N(3)-Pt(2)-N(A)	90.7 (9)
N(1)-Pt(1)-O(B)	86.7 (8)	N(3)-Pt(2)-N(B)	179.5 (8)
N(2)-Pt(1)-O(A)	87.0 (8)	N(4)-Pt(2)-N(A)	177.8 (10)
N(2)-Pt(1)-O(B)	174.4 (9)	N(4)-Pt(2)-N(B)	89.2 (8)
O(A)-Pt(1)-O(B)	95.2 (7)	N(A)-Pt(2)-N(B)	89.8 (8)
Pt(1)-O(A)-C(A1)	130 (2)	Pt(1)-O(B)-C(B1)	127 (2)
Pt(2)-N(A)-C(A1)	125 (2)	Pt(2)-N(B)-C(B1)	127 (2)
Pt(2)-N(A)-C(A4)	120 (2)	Pt(2)-N(B)-C(B4)	122 (2)
C(A1)-N(A)-C(A4)	115 (3)	C(B1)-N(B)-C(B4)	111 (2)
O(A)-C(A1)-N(A)	126 (3)	O(B)-C(B1)-N(B)	127 (2)
N(A)-C(A1)-C(A2)	109 (3)	N(B)-C(B1)-C(B2)	112 (2)
C(A1)-C(A2)-C(A3)	103 (2)	C(B1)-C(B2)-C(B3)	105 (2)
C(A2)-C(A3)-C(A4)	105 (3)	C(B2)-C(B3)-C(B4)	107 (2)
N(A)-C(A4)-C(A3)	105 (3)	N(B)-C(B4)-C(B3)	104 (2)
	PF_6^- and NO_3^- Anions		
P(A)-F(A1)	1.56 (2)	P(B)-F(B1)	1.56 (3)
P(A)-F(A2)	1.57 (3)	P(B)-F(B2)	1.42 (2)
P(A)-F(A3)	1.57 (2)	P(B)-F(B3)	1.54 (3)
		P(B)-F(B4)	1.46 (2)
N(0)-O(N1)	1.11 (2)	P(B)-F(B5)	1.49 (2)
N(0)-O(N2)	0.79 (6)	P(B)-F(B6)	1.50 (2)
F(A1)-P(A)-F(A2)	91 (5)	F(B1)-P(B)-F(B2)	93 (2)
F(A1)-P(A)-F(A3)	89 (1)	F(B1)-P(B)-F(B3)	177 (1)
F(A1)-P(A)-F(A1^{ii})		F(B1)-P(B)-F(B4)	95 (2)
F(A1)-P(A)-F(A2^{ii})		F(B1)-P(B)-F(B5)	85 (2)
F(A1)-P(A)-F(A3^{ii})		F(B1)-P(B)-F(B6)	87 (2)
F(A2)-P(A)-F(A3)	91 (1)	F(B2)-P(B)-F(B3)	89 (2)
F(A2)-P(A)-F(A2^{ii})		F(B2)-P(B)-F(B4)	92 (2)
F(A2)-P(A)-F(A3^{ii})		F(B2)-P(B)-F(B5)	88 (2)
F(A3)-P(A)-F(A3^{ii})		F(B2)-P(B)-F(B6)	176 (2)
		F(B3)-P(B)-F(B4)	87 (2)
O(N1)-N(0)-O(N2)	109 (2)	F(B3)-P(B)-F(B5)	93 (2)
O(N1)-N(0)-O(N1^{iii})	142 (4)	F(B3)-P(B)-F(B6)	92 (2)
		F(B4)-P(B)-F(B5)	179 (2)
		F(B4)-P(B)-F(B6)	92 (2)
		F(B5)-P(B)-F(B6)	87 (2)

[a] Symmetry operations: (i) $^1/_2 - x$, $^1/_2 - y$, $-z$; (ii) $1 - x$, y, $^3/_2 - z$; (iii) $-x$, y, $-^1/_2 - z$.

and angles within the coordination planes are comparable in both α-pyridonate and α-pyrrolidonate complexes of $Pt^{2.0+}$, the present complex diplays significantly longer Pt–Pt distances. Especially the outer Pt(1)–Pt(2) distance of 3.033 (2) Å is remarkably longer than the α-pyridonate-bridged Pt–Pt distance found in tetranuclear complexes of $Pt^{2.0+}$. Another example of an amidate bridged Pt–Pt distance in a Pt(II) complex is 3.131 Å in the hydantoinate complex.[13] The tilt angle (τ) between the Pt(1) and Pt(2) coordination planes increases as the Pt–Pt distance increases, as observed from the comparison of the pairs α-pyrrolidonate-tan and -yellow and α-pyridonate-blue and -yellow. The relationship between the tilt angle (τ) and the Pt–Pt distance among similar amidate-bridged complexes has been already reported[15] and is understood on the basis of simple geometric arguments that since the N---O bite distance in amide ligands is invariable regardless of the Pt–Pt distance, the tilt angle is increased as the Pt–Pt distance increases.

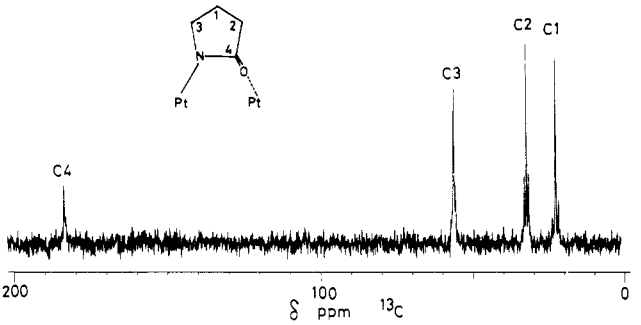

Figure 3. ^{13}C NMR spectrum of $[Pt_2(NH)_4(C_4H_6NO)_2]^{2+}$ in D_2O, measured on a JEOL FX90A spectrometer.

The larger tilt angle (τ) is also reflected in the smaller Pt–Pt–Pt zigzag chain angle. From the comparison of the tilt angles and the zigzag chain angles in Table III, it is obvious that as the tilt angle is increased, the zigzag chain angle is decreased in a pair of identical amide ligand complexes with different platinum oxidation states. This relation is also expressed in another way by saying that the tilt angle is decreased with increasing platinum average oxidation state.

^{13}C and ^{195}Pt NMR Studies. The ^{13}C NMR spectrum of the present compound in D_2O obtained on a JEOL FX90A spectrometer shows four peaks, the assignment of each signal being shown in Figure 3. Although four peaks seemingly appear in Figure 3, enlargement of the spectrum revealed that each peak consists actually of two closely lying peaks with almost equivalent intensities (C1, 21.76 and 21.62 ppm; C2, 31.21 and 31.17 ppm; C3, 55.40 and 55.17 ppm; C4, 182.55 and 182.28 ppm) (Figure 4, upper peaks). This fact demonstrates that the complex is composed of two similar species at a nearly 1:1 abundance ratio. These four peaks were also measured on a Bruker AC200P spectrometer in order to obtain information on the differences between the two components (Figure 4, lower peaks). Every signal broadens at its foot, showing possible splitting, and among them, the C2 peak is almost illustrative of a triplet with an approximate intensity ratio of 1:3:1: (theoretical ratio 1:4:1), which is due to the coupling with ^{195}Pt ($I = ^1/_2$, natural abundance = 33.7%). The coupling constant of 33.6 Hz for $^3J(^{195}Pt-^{13}C)$ is obtained. Some ^{195}Pt satellites also appear for other carbon atoms, but they are less clearly resolved especially in the case of 50.3 MHz (AC200P) than 22.5 MHz (FX90A). This satellite broadness is due to CSA relaxation of the ^{195}Pt nucleus.[17] As pointed out already,[18] ^{195}Pt relaxation becomes faster at higher fields of the observed frequency, which results in the broadness of the line width of ^{195}Pt satellite signals.

The ^{195}Pt NMR spectrum in D_2O shows three peaks at −1396, −1940, and −2446 ppm (Figure 5). The three peaks are not a splitting due to ^{195}Pt, considering the wide separation of the outer two peaks (ca. 19350 Hz). Recent ^{195}Pt NMR studies on a similar amide-bridged Pt(II) binuclear complex, $[Pt_2(en)_2(C_5H_4NO)_2]^{2+}$ ($C_5H_4NO^-$ is deprotonated α-pyridone), shows that the complex is binuclear in solution, although it is tetranuclear in crystal. Further remarkable behavior of the complex in an aqueous solution is that although the dimer is head-to-head immediately after dissolution in water, it is gradually converted to the head-to-tail isomer and the two isomers coexist in equilibrium after sufficient time.[4]

Considering the isomerization and the similar appearance of the three ^{195}Pt peaks of both complexes in $\delta(^{195}Pt)$ values, the three peaks in Figure 5 also show similar isomerization and the outer two peaks belong to the head-to-head isomer. The low- and high-field resonances of the head-to-head isomer are assigned to the N_2O_2- and N_4-coordinated platinum atoms, respectively, on the basis of established ^{195}Pt chemical shift trends.[19,20] The notable

(17) Lallemand, J.; Soulié, J.; Chottard, J. *J. Chem. Soc., Chem. Commun.* **1980**, 436.
(18) Anklin, C.; Pregosin, P. S. *Magn. Reson. Chem.* **1985**, *23*, 671.
(19) Lippard, S. J. *Science (Washington, D.C.)* **1982**, *218*, 1075.

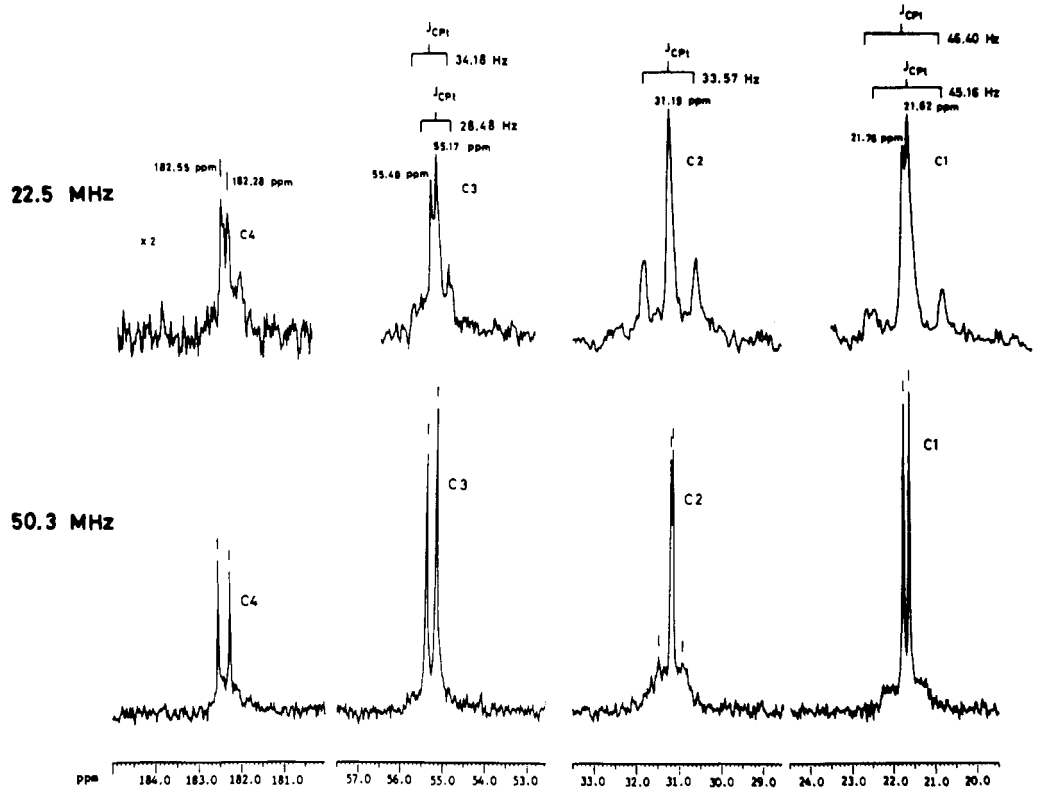

Figure 4. Enlargement of the four ^{13}C NMR peaks in Figure 3 (JEOL FX90A, at 22.5 MHz, upper four peaks) and the same peaks measured on a Bruker AC200P spectrometer, at 50.3 MHz (lower four peaks). The two closely lying peaks for each carbon show the existence of H-H and H-T isomers.

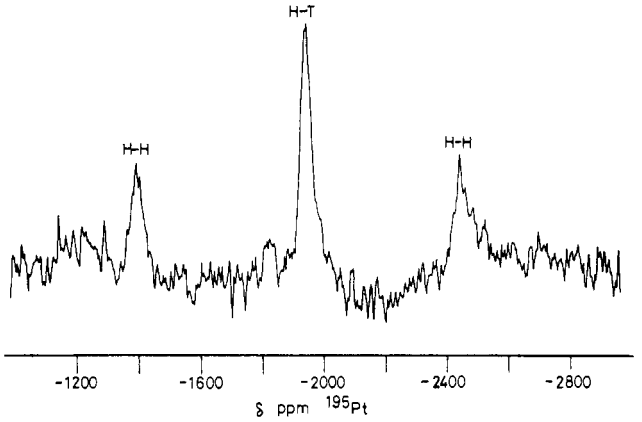

Figure 5. ^{195}Pt NMR spectrum of $[Pt_2(NH_3)_4(C_4H_6NO)_2]^{2+}$ in D_2O, showing the existence of H-H and H-T isomers.

difference between the present α-pyrrolidonate Pt(II) dimer and the α-pyridonate Pt(II) dimer is that the isomerization equilibrium seems to be established rapidly after dissolution for the former, whereas for the latter complex, $[Pt_2(en)_2(C_5H_4NO)_2]^{2+}$, equilibrium requires about 2 days to be established.[4] These observations are thoroughly consistent with the results of the ^{13}C NMR spectrum. The ^{195}Pt measurement of the present compound was repeated twice with different ellapsed times, immediately and 2 weeks after dissolution of the H-H dimer, but the peak intensity ratios of the central to the outer two peaks were the same. Also, the intensity ratios were compared for a solution prepared by dissolution of the H-H dimer and a solution in situ prepared by reducing $[Pt_4(NH_3)_8(C_4H_6NO)_4](NO_3)_6{\cdot}2H_2O$ with OH^-. No difference was observed in the peak positions and the signal intensity ratios. Therefore, it seems that H-H to H-T isomerization occurs very rapidly on addition of OH^- to $[Pt_4(NH_3)_8(C_4H_6NO)_4]^{6+}$. On slow evaporation of the solution after addition of $NaPF_6$, the H-H isomer crystallizes first because of its lower solubility. Since in Me_2SO the isomerization is reported to be very much retarded,[4] a ^{195}Pt NMR measurement of the present complex in Me_2SO was attempted; however, it was not successful due to the sparing solubility of the complex.

Very rapid isomerization of the present complex might be rather surprising, compared to the previously reported gradual one for the α-pyridonate Pt(II) dimer.[4] The difference may result from the difference in the keto–enol equilibria between α-pyrrolidone and α-pyridone. It seems the equilibrium lies more toward an enol form in α-pyridone, as shown by the existence of mononuclear Pt(II) complexes of 2-hydroxypyridine,[24] and therefore the coordinating ability of the deprotonated oxygen in α-pyridonate would be larger than that of α-pyrrolidonate. This difference might at least partly be responsible for the marked difference in the isomerization rates of the two complexes.

Although Figure 4 is the first observation of H-H and H-T isomers with ^{13}C NMR spectroscopy, the assignment of each peak in the each pair to either isomer is still uncertain. One may think, from the splitting intensity difference and the $J(^{195}Pt-^{13}C)$ coupling constants for C1 and C3, that, since the higher peak always associates with smaller coupling constants in both C1 and C3, the higher peak is H-T and the lower peak is H-H. This statement is based on the theory that a coupling constant is in proportion to the square of the electron densities at both nuclei[21] and, comparing H-H and H-T isomers, electron density at platinum would be higher for the N_4-coordinated platinum atom in the H-H isomer than for the N_3O-coordinated platinum atom in the H-T isomer. However, more evidence is necessary to make definite assignments of the two isomers in the ^{13}C NMR spectra. Several attempts were made to resolve ^{195}Pt satellites for C4; however, no further improvement was obtained.

The cyclic voltammogram of the present H-H complex in 4.5 M H_2SO_4 shows a single redox wave at $E_p = 0.53$ V vs SCE ($E_p = (E_{pa} + E_{pc})/2$), which is completely similar to the voltammogram reported for $[Pt_2(NH_3)_4(C_4H_6NO)_2]^{2+}$ in ref 1. In bulk

(20) Kerrison, S. J. S.; Sadler, P. J. *J. Magn. Reson.* **1978**, *31*, 321.
(21) Pregosin, P. S. *Annu. Rep. NMR Spectrosc.* **1986**, *17*, 295.
(22) Matsumoto, K.; Watanabe, T. *J. Am. Chem. Soc.* **1986**, *108*, 1308.
(23) Matsumoto, K.; Matoba, N. *Inorg. Chim. Acta* **1988**, *142*, 59.
(24) Hollis, L. S.; Lippard, S. J. *Inorg. Chem.* **1983**, *22*, 2708.

oxidative electrolysis of the solution at 0.8 V, the initially yellow solution turned blue, then gradually dark red, and finally yellow. This color change corresponds to the oxidation of yellow $[Pt_2(NH_3)_4(C_4H_6NO)_2]^{2+}$ to blue $[Pt_4(NH_3)_8(C_4H_6NO)_4]^{5+}$ and dark red $[Pt_4(NH_3)_8(C_4H_6NO)_4]^{6+}$ and finally to yellow $[Pt_4(NH_3)_8(C_4H_6NO)_4]^{8+}$,[22] which was confirmed by UV-visible absorption spectra. Bulk coulometry of the solution shows that the single wave at 0.53 V corresponds to a 4-electron redox process as a whole. The peak separation between E_{pc} and E_{pa} in the cyclic voltammogram could not be decreased less than 0.07 V at any scan rate from 0.001 to 0.5 V s^{-1}. A separate electrochemical study of $[Pt_4(NH_3)_8(C_4H_6NO)_4]^{6+}$ shows the cation also undergoes a single redox process at 0.53 V.[23] These facts, together with the color change during the bulk electrolysis of $[Pt_2(NH_3)_4(C_4H_6NO)_2]^{2+}$ and the very rapid isomerization from H-H to H-T, suggest that the redox reaction of $[Pt_2(NH_3)_4(C_4H_6NO)_2]^{2+}$ at 0.53 V is irreversible and consists actually of two or more very closely lying processes. The appearance of blue color in the bulk oxidative electrolysis signifies that at least the first oxidative step would be a 1- or 2-electron process

$$[Pt_2(NH_3)_4(C_4H_6NO)_2]^{2+} \xrightarrow{-e^-} [Pt_2(NH_3)_4(C_4H_6NO)_2]^{3+}$$

or

$$[Pt_2(NH_3)_4(C_4H_6NO)_2]^{2+} \xrightarrow{-2e^-} [Pt_2(NH_3)_4(C_4H_6NO)_2]^{4+}$$

The blue $[Pt_4(NH_3)_8(C_4H_6NO)_4]^{5+}$ cation would be formed by either one of the two following reactions:

$$[Pt_2(NH_3)_4(C_4H_6NO)_2]^{3+} + [Pt_2(NH_3)_4(C_4H_6NO)_2]^{2+} \rightarrow [Pt_4(NH_3)_8(C_4H_6NO)_4]^{5+}$$

$$[Pt_2(NH_3)_4(C_4H_6NO)_2]^{4+} + 3[Pt_2(NH_3)_4(C_4H_6NO)_2]^{2+} \rightarrow 2[Pt_4(NH_3)_8(C_4H_6NO)_4]^{5+}$$

It seems that H-H and H-T $[Pt_2(NH_3)_4(C_4H_6NO)_2]^{2+}$ isomers have very close or almost identical redox potentials or oxidation of either isomer triggers very rapid isomerization and the oxidation proceeds almost exclusively via either one of the isomers. It also seems that some isomerization occurs following oxidation of the compound, since the cyclic voltammogram becomes less reversible with the peak separation between E_{pa} and E_{pc} being increased, though the E_p potential is retained, as the acidity of the solution is decreased.

Conclusion

Lippard et al. reported a possible relationship between structural features, such as the Pt-Pt distance and the torsional angle about the Pt-Pt vector, and the ease of linkage isomerization.[4] The long Pt-Pt distance in the present complex may result in the rapid isomerization of the complex. However, the torsional angle in this complex is not so large; therefore, it seems that rapid isomerization does not always result from strong torsional strain. The isomerization seems also to be related to the nature of the amide ligand. The relative contributions of the keto and enol forms of the amidate ligand influence the relative degrees of the coordinating abilities of amidate oxygen and nitrogen atoms and thus affect the isomerization rate.

The present study clarified the solid and solution structures of a *cis*-diammineplatinum(II) α-pyrrolidonate complex, which was synthesized by the reduction of the tetranuclear Pt(II) and Pt(III) mixed-valent complex $[Pt_4(NH_3)_8(C_4H_6NO)_4]^{6+}$.

Acknowledgment. We are indebted to the Toray Science Foundation and Japanese Ministry for Health and Welfare for their financial support.

Registry No. $[Pt_2(NH_3)_4(C_4H_6NO)_2]_2(PF_6)_3(NO_3)\cdot H_2O$, 119942-98-2; ^{195}Pt, 14191-88-9.

Supplementary Material Available: Anisotropic thermal parameters (Table S2) (1 page); final observed and calculated structure factors (Table S1) (19 pages). Ordering information is given on any current masthead page.

Contribution from the Departments of Chemistry, Queens College-City University of New York, Flushing, New York 11367-0904, and University of Houston, Houston, Texas 77204-5641

Resonance Raman Spectra and Excited-State Lifetimes for a Series of 3,3′-Polymethylene-2,2′-bipyridine Complexes of Ruthenium(II)

Thomas C. Strekas,*,† Harry D. Gafney,† Steven A. Tysoe,† Randolph P. Thummel,*,‡ and Francois Lefoulon‡

Received December 6, 1988

The complexes RuL_3^{2+}, where L is a 3,3′-polymethylene-2,2′-bipyridine ligand containing one to four bridging methylene units, were studied by using resonance-enhanced Raman spectroscopy. Lifetimes and emission spectra were measured at room temperature and at 77 K. Complexes with the monomethylene-bridged ligand show results distinctly different from those of the dimethylene-, trimethylene-, and tetramethylene-bridged ligand complexes, which form a series showing systematic variations in the resonance Raman and emission spectra that correlate with the degree to which the polymethylene bridge distorts the planarity of 2,2′-bipyridine. As the bridge length increases, the relative quantum yield for emission at 25 °C drops. Twisting about the 2,2′-bond may result in a weakening of the ligand field leading to lower lying ligand field states, which provide a route for more facile radiationless deactivation. Both the relative intensity pattern in the resonance Raman spectra and the intensities of the low-energy shoulders in the 77 K emission spectra suggest an increase in the number of ligand normal modes capable of efficiently coupling ground and excited states as the number of methylene units increases from 2 to 4. This is consistent with increased rates for nonradiative deexcitation, most likely through these same high-frequency "acceptor" modes.

Introduction

The effect of varying steric and electronic factors in diimine type ligands on the properties of their ruthenium(II) complexes remains an active area of investigation.[1] Because of the capability of $Ru(bpy)_3^{2+}$ (bpy = 2,2′-bipyridine) to act as an excited-state redox reagent,[2] the degree to which ligand properties can influence the excited-state properties of these complexes is of considerable interest.

Recently reported[3] NMR and X-ray data concerning the ruthenium(II) complexes of a series of 3,3′-polymethylene-bridged

† Queens College.
‡ University of Houston.

(1) (a) Thummel, R. P.; Lefoulon, F. *Inorg. Chem.* **1987**, *26*, 675. (b) Thummel, R. P.; Decloitre, Y.; Lefoulon, F. *Inorg. Chim. Acta* **1987**, *128*, 245. (c) Binamira-Soriga, E.; Sprouse, S. D.; Watts, R. J.; Kaska, W. C. *Inorg. Chim. Acta* **1984**, *84*, 135. (d) Klassen, D. M. *Inorg. Chem.* **1976**, *15*, 3166. (e) Anderson, S.; Seddon, K. R.; Wright, R. D. *Chem. Phys. Lett.* **1980**, *71*, 220. (f) Allen, G. H.; White, R. P.; Rillema, D. P.; Meyer, T. *J. Am. Chem. Soc.* **1984**, *106*, 2613. (g) Balzani, V.; Juris, A.; Barigelletti, F.; Belser, P.; von Zelewsky, A. *Sci. Pap. Inst. Phys. Chem. Res. (Jpn.)*. **1984**, *78*, 78. (h) Belser, P.; von Zelewsky, A. *Helv. Chim. Acta.* **1980**, *63*, 1675. (i) Belser, P.; von Zelewsky, A. *Chem. Phys. Lett.* **1982**, *89*, 101.

0020-1669/89/1328-2964$01.50/0